J.Serb.Chem.Soc. *68*(4–5)363–381(2003) UDC 547.314.2:533.912:512.57
JSCS – 3052 *Original scientific paper*

Use of the group theory for classification of electronic states of acetylene*

STANKA JEROSIMIĆ and MILJENKO PERIĆ

Faculty of Physical Chemistry, University of Belgrade, Studentski trg 16, 11000 Belgrade, Serbia and Montenegro

(Received 15 July 2002)

Abstract: The electronic states of the acetylene molecule are classified employing the group theory combined with the use of the Walsh diagrams and some elementary quantum chemical considerations. The results of this analysis are compared with those obtained by explicit *ab initio* calculations. It is shown that the global structure of the electronic spectrum can be reproduced/predicted without carrying out detailed *ab initio* calculations.

Keywords: group theory, Walsh diagrams, classification of electronic states, acetylene.

INTRODUCTION

It is well known that the group theory represents a very powerful tool for the classification of electronic, vibrational and rotational states of molecules, particularly those possessing highly symmetrical nuclear configurations.[1,2] A serious drawback of this approach is, however, that the corresponding statements are generally of only qualitative nature. So, for example, on the basis of symmetry considerations alone the number and type of electronic states arising by various populations of a set of molecular orbitals can be predicted, but not their energy ordering or the energy difference between them. In the present paper, it will be shown that also a lot of semiquantitative information can be obtained if pure group theory results are combined with some elementary quantum chemical considerations. This will be illustrated on the example of the acetylene molecule. This species was chosen for two reasons: firstly, it is interesting from the group theoretical point of view because of its relatively high symmetry (taking into account the small number of atoms) and the fact that the equilibrium geometries in its various electronic states belong to different point groups ($D_{\infty h}$, C_{2h}, C_{2v}, C_2, ...); secondly, the importance of this molecule may make the results of the present analysis interesting not only from a pure methodological point of view.

The present approach is of course not new. Its roots represent the well known Mulliken–Walsh rules[3,4] which enable a number of qualitative and even semiquantitative

* Dedicated to Professor Miroslav J. Gašić on the occasion of his 70th birthday.

predictions concerning the geometry and energy ordering of electronic states of various classes of molecules to be made. We shall shorten here this name to Walsh rules, in spite of the fact that particularly in Mulliken's hands this simple and elegant model has led to fascinating results; the reason for this is that there are also many other "Mulliken's rules" in this and related topics. The Walsh rules were derived in the precomputer era on the basis of simple MO-LCAO (molecular orbital as linear combination of atomic orbitals) considerations. The use of computers for solving the molecular Hartree–Fock (HF) equations has enabled the quantitative generation of the entities (molecular orbitals and the corresponding orbital energies) entering the Walsh model (see, *e.g.*, Ref. 5). Although this "quantification" of the model introduces several new problems, not existing, or at least being hidden, from the pure qualitative point of view (see, *e.g.*, Ref. 6), there are at least two important advantages thereof: 1) it explains some important features not understandable on the basis of the qualitative MO theory alone; b) it represents an important link between naive concepts and the results of explicit *ab initio* calculations, the latter being of high (numerical) accuracy but are given in terms of very complex energy surfaces and corresponding wave functions, which obscures their interpretation.

MO DIAGRAMS FOR HAAH MOLECULES

In a previous paper,[7] the behavior of MOs for the class of molecules with the formula HAAH, where A represents an atom belonging to the first row of the periodic table (*e.g.*, B, N, O), at the H–A and A–A stretching was discussed. In the present study are considered the angular (bending and torsional) dependence of the same quantities. To simplify the situation, it is assumed that all the bond lengths are kept fixed at their equilibrium values. At nuclear arrangements corresponding to these types of distortions with respect to the linear geometry ($D_{\infty h}$ point group) the molecule belongs to various point groups: C_{2h} (at the *trans*-bending), $C_{2\upsilon}$ (*cis*-bending), C_2 (torsion at equal H–A–A bond angles). The correlation between the irreducible representations (irreps) of these point groups is given in Table I. For sake of completeness, the group C_s is also presented. The choice of the axes is made according to the usual convention: For $D_{\infty h}$ the *z*-axis coincides with the molecular axis, for C_{2h}, $C_{2\upsilon}$ and C_2 it represents the C_2 symmetry axis, and for C_s it is perpendicular to the symmetry (molecular) plane. In all cases except for $D_{\infty h}$ the *y*-axis is taken to lie along the A–A bond.

For the discussion which follows it is convenient to first construct for each point group of interest the symmetrized linear combinations of the atomic orbitals (AO) building the "minimal" AO basis for the systems considered. The minimal AO basis consists of the following species:

$$\begin{gathered} 1s_A\,,\, 2s_A\,,\, 2p_{xA} \equiv x_A\,,\, 2p_{yA} \equiv y_A,\, 2p_{zA} \equiv z_A\,, \\ 1s_B\,,\, 2s_B\,,\, 2p_{xB} \equiv x_B\,,\, 2p_{yB} \equiv y_B\,,\, 2p_{zB} \equiv z_B\,, \\ 1s_{HA} \equiv s_{HA}\,,\, 1s_{HB} \equiv s_{HB}\,. \end{gathered} \tag{1}$$

In Eq. 1 different symbols (A, B) for the two heavy atoms and the two hydrogens (H_A, H_B) are introduced. In this new notation the HAAH molecule reads H_A A B H_B. The symmetric and antisymmetric linear combination of pairs of these twelve AOs build the bases for irreducible representations of the point groups in question, as given in Table II. Note that the symmetry species appearing in the same row of Table II do *not* necessarily correlate with one another (*e.g.*, π_u, b_u+b_u, b_1+b_2, b+b, corresponding to the two-dimensional space spanned by x_A+x_B and y_A+y_B), because of the different meaning of the x, y, and z axes for the different point groups. In the C_s point group each individual AO, except for z_A and z_B belongs to a', the latter two being of a" symmetry.

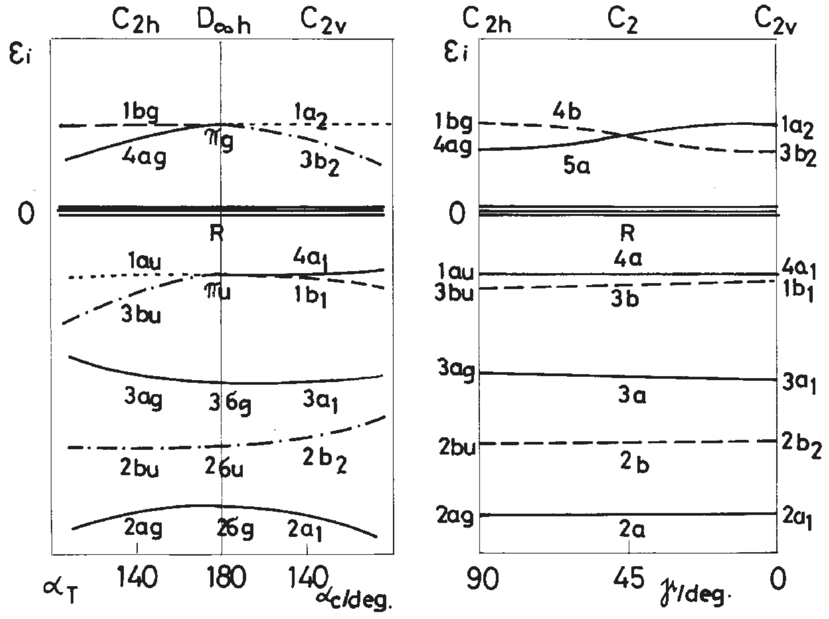

a b

Fig. 1. The dependence of MO energies on variation of geometry in symmetric tetraatomic molecules HAAH. 1a: *Trans*- and *cis*-bending. Solid lines denote species of a_g (C_{2h} point group) and a_1 (C_{2v} group) symmetry, dotted lines a_u and a_2, dashed lines b_g and b_1, dash-dotted lines b_u and b_2. 1b: Torsional dependence of MO energies. Solid lines denote species of **a** symmetry, dashed lines **b** MOs. Correlation of C_2 species with their C_{2h} and C_{2v} counterparts is indicated.

Besides these twelve ("valence") AOs, the s, p, ... Rydberg orbitals will also be considered, because the latter are involved in the series of experimentally observed excited electronic states of the acetylene molecule. These orbitals are characterized by large spatial extension and closely resemble the orbitals of an isolated atom. They can all be assumed to be centered at the mid-point of the molecule and each of them transforms separately according to the total-symmetrical irrep (s-species), like the x, y, z coordinates (p_x, p_y, p_z Rydberg orbitals, respectively), *etc.*, in each of the point groups considered.

TABLE I. Correlation of the species of a linear molecule ($D_{\infty h}$ point group) with those of a molecule of lower symmetry.

$D_{\infty h}$	C_{2h}	C_{2v}	C_2	C_s
Σ_g^+	A_g	A_1	A	A’
Σ_g^-	B_g	B_1	B	A"
Π_g	$A_g + B_g$	$A_2 + B_2$	A + B	A’ + A"
Δ_g	$A_g + B_g$	$A_1 + B_1$	A + B	A’ + A"
Φ_g	$A_g + B_g$	$A_2 + B_2$	A + B	A’ + A"
...	...	...	...	...
Σ_u^+	B_u	B_2	B	A’
Σ_u^-	A_u	A_2	A	A"
Π_u	$A_u + B_u$	$A_1 + B_1$	A + B	A’ + A"
Δ_u	$A_u + B_u$	$A_2 + B_2$	A + B	A’ + A"
Φ_u	$A_u + B_u$	$A_1 + B_1$	A + B	A’ + A"
...	...	...	...	...

TABLE II. Classification of atomic orbitals according to the irreducible representations of the point groups of interest.

	$D_{\infty h}$	C_{2h}	C_{2v}	C_2
$1s_A + 1s_B$	σ_g	a_g	a_1	a
$1s_A - 1s_B$	σ_u	b_u	b_2	b
$2s_A + 2s_B$	σ_g	a_g	a_1	a
$2s_A - 2s_B$	σ_u	b_u	b_2	b
$x_A + x_B$	π_u	b_u	b_1	b
$y_A + y_B$		b_u	b_2	b
$z_A + z_B$	σ_u	a_u	a_1	a
$x_A - x_B$	π_g	a_g	a_2	a
$y_A - y_B$		a_g	a_1	a
$z_A - z_B$	σ_g	b_g	b_2	b
$H_A + H_B$	σ_g	a_g	a_1	a
$H_A - H_B$	σ_u	b_u	b_2	b

The dependence of the energies of the low-energy orbitals up to $1\pi_g$ (except for the $1\sigma_g$ and $1\sigma_u$ which are characterized by much lower energies than those of all other species) on the bending coordinates is presented in Fig. 1a. It is extracted from HF calculations on several HAAH molecules and is in most, but not all instances, qualitatively the same as that predicted in the original studies by Mulliken and Walsh. The data of Fig. 1a is of semiquantitative nature in the sense that the energy ordering, increase or decrease of the curves are reproduced quite correctly, while the energy differences between the curves are arbitrary.

First the composition of the MOs for the linear nuclear arrangement will be discussed. The two MOs with the lowest energy, $1\sigma_g$ and $1\sigma_u$ (not shown in Fig. 1a), are built by the symmetric and antisymmetric linear combinations of the 1s AOs of the A, B atoms. The electrons populating these orbitals are mainly localized at the heavy nuclei and do not contribute significantly to the binding of the atoms in the molecule. The next two orbitals in order of increasing energy are $2\sigma_g$ and $2\sigma_u$, composed predominately by the symmetric and antisymmetric linear combinations of the 2s A, B orbitals, respectively, with a small admixture of the hydrogen 1s AOs. They are followed by $3\sigma_g$, involving the antisymmetric linear combination of the $2p_z$ A, B orbitals directed along the molecular axis ($2p\sigma$) and the symmetric linear combination of the hydrogen 1s AOs. The next orbital is $1\pi_u$, composed of the symmetric linear combination of the p orbitals of the A, B atoms perpendicular to the molecular axis ($2p_x$, $2p_y = 2p\pi$). If the AO basis employed did not involve the Rydberg-type species, the lowest-lying orbitals not occupied in the ground state of C_2H_2 ("virtual orbital") would be $1\pi_g$, built by the symmetric linear combinations of the $2p\pi$ A, B AOs. It would be followed by the $3\sigma_u$ orbital, *etc*. However, the Rydberg orbitals present in the AO basis employed enter into a branch of non-bonding MOs, characterized with energies close to zero, and lying thus between $1\pi_u$ and $1\pi_g$. Let us note that discrete energies of virtual orbitals are actually artificial; if the AO basis were infinite, the spectrum of virtual orbitals would be continuous.

The behaviour of the orbital energies upon bending is governed by several effects. First of all, because of the reduced symmetry, all the species doubly degenerate in the linear geometry (π, δ, ...) split into two components. The second important effect is that in the lower-symmetry groups more AOs are generally involved in a MO belonging to a particular irrep, which can contribute to a lowering of its energy - an example for this are the $2a_g$ and $2a_1$ orbitals compared with $2\sigma_g$ to which they correlate in the linear nuclear arrangement. The overlap between the AOs belonging to a hydrogen and a heavy atom within a MO can become more (as, for example, in $3b_u$) or less (*e.g.*, in $3a_g$ and $3a_1$) pronounced upon bending; in the first case such a MO is stabilized, in the second case it is destabilized upon bending. The next effect influencing the geometry dependence of orbital energies is mutual "repelling" of MOs of the same symmetry and similar energy (as *e.g.*, $3a_1$ and $4a_1$). Finally, the composition of MOs and consequently their energy is influenced by the requirement for their mutual orthogonality. The form of the curves presented in Fig. 1a can be interpreted more or less straightforwardly by taking into account all these facts (see also Ref. 5). The behavior of the MOs involving also Rydberg-type AOs is clearly dominated by the properties of these species; these MOs show no significant change in composition and energy with variation of the geometry.

In. Fig. 1b are displayed the orbital energies as functions of the torsion angle at a particular value for the bending angle $\angle$ H_A–A–B = $\angle$ A–B–H_B (of, say 120º). The torsion angle γ is defined as half the angle between the H_AAB and ABH_B planes. This means that $\gamma = 0$ for *cis*-planar geometry, and $\gamma = \pi/2$ for *trans*-planar nuclear arrangement. Only the 5a and 4b orbitals show significant change upon torsion. This is easy to explain: The 5a orbital correlates at *trans*-planar geometry ($\gamma = \pi/2$) with the $4a_g$ species; this MO is predominantly built by the antisymmetric linear combination of the p_x orbitals of the heavy atoms (lying in the molecular plane), but is significantly admixed by the symmetric linear combination of the hydrogen 1s function. The overlap between these functions decreases with decreasing torsional angle. At *cis*-planar geometry, the 5a orbital correlates with $1a_2$, the latter does not involve the hydrogen AOs for symmetry reasons (see Table II). A consequence of these facts is that the energy of the 5a orbital decreases on changing of the molecular geometry from *trans*-planar towards *cis*-planar. The behavior of the 4b species is just the opposite.

VERTICAL ELECTRONIC SPECTRUM OF ACETYLENE

In the ground electronic state, the acetylene molecule is linear. The electronic configuration of the ground state corresponds to the distribution of fourteen electrons among the lowest-energy MOs available: $1\sigma_g^2\ 1\sigma_u^2\ 2\sigma_g^2\ 2\sigma_u^2\ 3\sigma_g^2\ 1\pi_u^4$. The symmetry of this state is thus $^1\Sigma_g^+$.

The lowest-lying excited state of acetylene corresponds to a one-electron excitation from the highest MO populated in the ground state $1\pi_u \equiv \pi_u$, into the lowest lying unpopulated ("virtual") MO, $1\pi_g \equiv \pi_g$ ($\pi_u^3\ \pi_g$ configurations). When considering the linear nuclear arrangement, it is convenient to use instead of Cartesian components of these orbitals their linear combinations which are eigenfunctions of the projection of the electronic angular momentum operator onto the molecular axis, L_z. All the electronic configurations which are considered in the present study have at most two electrons in "open shells", *i.e.*, in (spatial) orbitals populated with a single electron (at linear geometry there will actually also be situations where three electrons occupy a π orbital – such a case can and shall be treated as a single "hole" in this MO). Since the electrons occupying "closed shells" do not contribute to the molecular angular (spatial and spin) momentum, the *z*-components of the angular momentum and spin operator of the molecule can be written in the form

$$L_z = l_{z1} + l_{z2} = -\mathrm{i}\left(\frac{\partial}{\partial\phi_1} + \frac{\partial}{\partial\phi_2}\right);\ S_z = s_{z1} + s_{z2} \tag{2}$$

(atomic units, $m_e \equiv 1$, $e \equiv 1$, $\hbar \equiv 1$ are used throughout this paper) where indices 1 and 2 denote the electrons which can be outside the closed shells, and ϕ_1, ϕ_2 represent their azimuthal angles. To obtain the required components of the π orbitals one starts with the p AOs of the heavy atoms (A, B) expressed in polar coordinates,

$$\begin{aligned} 2p_{xA} &\equiv x_A = f(\rho, z_A)\cos\phi, \quad 2p_{xB} \equiv x_B = f(\rho, z_B)\cos\phi, \\ 2p_{yA} &\equiv y_A = f(\rho, z_A)\sin\phi, \quad 2p_{yB} \equiv y_B = f(\rho, z_B)\sin\phi, \end{aligned} \tag{3}$$

where the symbol z_A (z_B) indicates that the corresponding function is centered at the nucleus A (B). It follows that

$$\begin{aligned} x_A + x_B &= f_u \cos\phi, \quad x_A - x_B = f_g \cos\phi, \\ y_A + y_B &= f_u \sin\phi, \quad y_A - y_B = f_g \sin\phi, \end{aligned} \tag{4}$$

where

$$f_u \equiv f(\rho, z_A) + f(\rho, z_B), \quad f_g \equiv f(\rho, z_A) - f(\rho, z_B). \tag{5}$$

Now the linear combinations of (4) are built,

$$\begin{aligned} \pi_u &= \frac{1}{2\sqrt{1+S}}\,[(x_A + x_B) + i\,(y_A + y_B)] = f_u\, e^{i\phi} \\ \bar{\pi}_u &= \frac{1}{2\sqrt{1+S}}\,[(x_A + x_B) - i\,(y_A + y_B)] = f_u\, e^{-i\phi} \\ \pi_g &= \frac{1}{2\sqrt{1-S}}\,[(x_A - x_B) + i\,(y_A - y_B)] = f_g\, e^{i\phi} \\ \bar{\pi}_g &= \frac{1}{2\sqrt{1-S}}\,[(x_A - x_B) - i\,(y_A - y_B)] = f_g\, e^{-i\phi} \end{aligned} \tag{6}$$

It is assumed that AOs are real and normalized (but, of course, not mutually orthogonal in the general case); S is the overlap integral,

$$S \equiv \int x_A\, x_B\, d\tau \equiv \int y_A\, y_B\, d\tau. \tag{7}$$

There are 16 Slater detrminants corresponding to the $\pi_u^3\, \pi_g$ configurations, which are in accordance with the Pauli principle:

$$\begin{aligned} &D_1 = |\bar{\pi}_u\alpha, \pi_g\alpha|, \; D_2 = |\bar{\pi}_u\alpha, \pi_g\beta|, \; D_3 = |\bar{\pi}_u\alpha, \bar{\pi}_g\alpha|, \; D_4 = |\bar{\pi}_u\alpha, \bar{\pi}_g\beta|, \\ &D_5 = |\bar{\pi}_u\beta, \pi_g\alpha|, \; D_6 = |\bar{\pi}_u\beta, \pi_g\beta|, \; D_7 = |\bar{\pi}_u\beta, \bar{\pi}_g\alpha|, \; D_8 = |\bar{\pi}_u\beta, \bar{\pi}_g\beta|, \\ &D_9 = |\pi_u\alpha, \pi_g\alpha|, \; D_{10} = |\pi_u\alpha, \pi_g\beta|, \; D_{11} = |\pi_u\alpha, \bar{\pi}_g\alpha|, \; D_{12} = |\pi_u\alpha, \bar{\pi}_g\beta|, \\ &D_{13} = |\pi_u\beta, \pi_g\alpha|, \; D_{14} = |\pi_u\beta, \pi_g\beta|, \; D_{15} = |\pi_u\beta, \bar{\pi}_g\alpha|, \; D_{16} = |\pi_u\beta, \bar{\pi}_g\beta|, \end{aligned} \tag{8}$$

The shortened notation for the Slater determinants will be employed, *e.g.*,

$$|\pi\alpha, \bar{\pi}\beta| \equiv \frac{1}{\sqrt{2}} \begin{vmatrix} \pi(1)\alpha(1) & \bar{\pi}(1)\beta(1) \\ \pi(2)\alpha(2) & \bar{\pi}(2)\beta(2) \end{vmatrix} \tag{9}$$

The electronic Hamiltonian of a linear molecule commutes with the operators L_z, S^2 and S_z, and thus the quantum numbers corresponding to these operators, Λ, S and M_S are "good" quantum numbers. All the Slater determinants (8) are eigenfunctions of L_z and S_z but generally not of S^2. Additionally, the Hamiltonian commutes with the operator for permutations of identical nuclei (A, B and H_A, H_B), as well as with the operator σ_υ corresponding to the reflection of all electronic spatial coordinates in the planes crossing one another along the molecular axis. Thus, a correct electronic wave function is labeled by the quantum number *g* or *u*, according to its behavior upon reflection in the nuclear inversion centrum, and the wave function for a Σ ($\Lambda = 0$) electronic states also by + if it is invariant upon reflection in σ_υ and by – if it changes sign under this operation. From the Slater determinants (8) the following spectroscopic states are constructed:

$$
\begin{aligned}
{}^1\Delta_u &= \frac{1}{\sqrt{2}}(D_{10}–D_{13}) = {}^1\Phi_2\,\Theta^1,\\
{}^1\overline{\Delta}_u &= \frac{1}{\sqrt{2}}(D_4–D_7) = {}^1\Phi_{-2}\,\Theta^1;\\
{}^3\Delta_u\,(M_S=1) &= D_9 = {}^3\Phi_2\,\Theta^3{}_1,\\
{}^3\Delta_u\,(M_S=0) &= \frac{1}{\sqrt{2}} = (D_{10}+D_{13}) = {}^3\Phi_2\,\Theta^3{}_0,\\
{}^3\Delta_u\,(M_S=-1) &= D_{14} = {}^3\Phi_2\,\Theta^3{}_{-1};\\
{}^3\overline{\Delta}_u\,(M_S=1) &= D_3 = {}^3\Phi_{-2}\,\Theta^3{}_1,\\
{}^3\overline{\Delta}_u\,(M_S=0) &= \frac{1}{\sqrt{2}}(D_4+D_7) = {}^3\Phi_{-2}\,\Theta^3{}_0,\\
{}^3\overline{\Delta}_u\,(M_S=-1) &= D_8 = {}^3\Phi_{-2}\,\Theta^3{}_{-1},\\
{}^1\Sigma_u{}^+ &= \frac{1}{2}(D_2-D_5+D_{12}-D_{15}) = {}^1\Phi^+\,\Theta^1,\\
{}^3\Sigma_u{}^+\,(M_S=1) &= \frac{1}{\sqrt{2}}(D_1+D_{11}) = {}^3\Phi^+\,\Theta^3{}_1,\\
{}^3\Sigma_u{}^+\,(M_S=0) &= \frac{1}{2}(D_2+D_5+D_{12}+D_{15}) = {}^3\Phi^+\,\Theta^3{}_0,\\
{}^3\Sigma_u{}^+\,(M_S=-1) &= \frac{1}{\sqrt{2}}(D_6+D_{16}) = {}^3\Phi^+\,\Theta^3{}_{-1};\\
{}^3\Sigma_u{}^- &= \frac{1}{2}(D_2-D_5-D_{12}+D_{15}) = {}^1\Phi^-\,\Theta^1,\\
{}^3\Sigma_u{}^-\,(M_S=1) &= \frac{1}{\sqrt{2}}(D_1-D_{11}) = {}^3\Phi^-\,\Theta^3{}_1,\\
{}^3\Sigma_u{}^-\,(M_S=0) &= \frac{1}{2}(D_2+D_5-D_{12}-D_{15}) = {}^3\Phi^-\,\Theta^3{}_0,\\
{}^3\Sigma_u{}^-\,(M_S=-1) &= \frac{1}{\sqrt{2}}(D_6-D_{16}) = {}^3\Phi^-\,\Theta^3{}_{-1}.
\end{aligned}
\tag{10}
$$

On the left-hand side Δ stands for the species with $\Lambda = 2$, $\overline{\Delta}$ for those corresponding to $\Lambda = -2$. The components of a triplet state are denoted by the value of M_S given in parentheses. The functions appearing in Eqs. (10) are defined as

$$
\begin{aligned}
{}^1\Phi_2 &\equiv \frac{1}{\sqrt{2}}\,[\pi_u(1)\,\pi_g(2)+\pi_g(1)\,\pi_u(2)] \equiv \frac{1}{\sqrt{2}}[\pi_u\pi_g+\pi_g\pi_u] = \\
&= \frac{1}{\sqrt{2}}\,[f_u(1)\,f_g(2)+f_g(1)\,f_u(2)]\,\exp[\mathrm{i}(\phi_1+\phi_2)] \equiv \frac{1}{\sqrt{2}}\,[f_uf_g+f_gf_u]\,\exp[\mathrm{i}(\phi_1+\phi_2)], \\
{}^1\Phi_{-2} &= \frac{1}{\sqrt{2}}\,[\bar{\pi}_u\bar{\pi}_g+\bar{\pi}_g\bar{\pi}_u] = \frac{1}{\sqrt{2}}\,[f_uf_g+f_gf_u]\,\exp[-\mathrm{i}(\phi_1+\phi_2)\,], \\
{}^3\Phi_2 &= \frac{1}{\sqrt{2}}\,[\pi_u\pi_g-\pi_g\pi_u] = \frac{1}{\sqrt{2}}\,[f_uf_g-f_gf_u]\,\exp[\mathrm{i}(\phi_1+\phi_2)\,], \\
{}^3\Phi_{-2} &= \frac{1}{\sqrt{2}}\,[\bar{\pi}_u\bar{\pi}_g-\bar{\pi}_g\bar{\pi}_u] = \frac{1}{\sqrt{2}}[f_uf_g-f_gf_u]\,\exp[-\mathrm{i}(\phi_1+\phi_2)\,], \\
{}^1\Phi^+ &= \frac{1}{2}\,[\pi_u\bar{\pi}_g+\bar{\pi}_g\pi_u+\bar{\pi}_u\pi_g+\pi_g\bar{\pi}_u] = [f_uf_g+f_gf_u]\,\cos(\phi_1-\phi_2)\,, \\
{}^3\Phi^+ &= \frac{1}{2}\,[\pi_u\bar{\pi}_g-\bar{\pi}_g\pi_u+\bar{\pi}_u\pi_g-\pi_g\bar{\pi}_u] = [f_uf_g-f_gf_u]\,\cos(\phi_1-\phi_2)\,, \\
{}^1\Phi^- &= \frac{1}{2}\,[\pi_u\bar{\pi}_g+\bar{\pi}_g\pi_u-\bar{\pi}_u\pi_g-\pi_g\bar{\pi}_u] = \mathrm{i}\,[f_uf_g-f_gf_u]\,\sin(\phi_1-\phi_2)\,, \\
{}^3\Phi^- &= \frac{1}{2}\,[\pi_u\bar{\pi}_g-\bar{\pi}_g\pi_u-\bar{\pi}_u\pi_g+\pi_g\bar{\pi}_u] = \mathrm{i}\,[f_uf_g+f_gf_u]\,\sin(\phi_1-\phi_2)\,,
\end{aligned} \tag{11}
$$

and

$$
\begin{aligned}
\Theta^1 &\equiv \frac{1}{\sqrt{2}}\,[\alpha(1)\,\beta(2)-\beta(1)\alpha(2)\,] \equiv \frac{1}{\sqrt{2}}\,(\alpha\beta-\beta\alpha) \\
\Theta^3{}_1 &= \alpha(1)\,\alpha(2) \equiv \alpha\alpha, \\
\Theta^3{}_0 &= \frac{1}{\sqrt{2}}\,[\alpha(1)\,\beta(2)+\beta(1)\,\alpha(2)] \equiv \frac{1}{\sqrt{2}}\,(\alpha\beta+\beta\alpha) \\
\Theta^3{}_{-1} &= \beta(1)\,\beta(2) \equiv \beta\beta\,.
\end{aligned} \tag{12}
$$

Now the approximate expectation values for the electronic Hamiltonian, corresponding to the wave functions defined by Eqs. (10), will be derived. It is assumed that the contribution from the closed shells is the same in all cases, and that the relative ordering of the states considered can be obtained by computing the mean value of the Hamiltonian for two electrons,

$$
H = h_1 + h_2 + \frac{1}{r_{12}} \tag{13}
$$

where h_1 and h_2 are one-electron operators and r_{12} is the distance between the electrons 1 and 2. The contribution from the one-electron operators h_1 and h_2 is for all the present cases ($\pi_u\pi_g$ configurations)

$$< \pi_u | h_{1/2} | \pi_u > + < \pi_g | h_{1/2} | \pi_g > \equiv \varepsilon_u + \varepsilon_g . \tag{14}$$

The mean values for the two-electron operator $1/r_{12}$ are

$$^1\Delta_u : J_{ug} + K_{ug} =$$
$$\frac{1}{2(1-S^2)}\{(x_A x_A \mid x_A x_A) - (x_A x_B \mid x_A x_B) + (x_A x_A \mid y_A y_A) - (x_A x_B \mid y_A y_B) +$$
$$+ (x_A y_B \mid x_A y_B) - (x_A y_B \mid x_B y_A)\},$$
$$^3\Delta_u : J_{ug} - K_{ug} =$$
$$\frac{1}{2(1-S^2)}\{(x_A x_A \mid x_B x_B) - (x_A x_B \mid x_A x_B) + (x_A x_A \mid y_B y_B) - (x_A x_B \mid y_A y_B) -$$
$$- (x_A y_B \mid x_A y_B) + (x_A y_B \mid x_B y_A)\},$$
$$^1\Sigma_u^+ : J_{u\bar{g}} + K_{u\bar{g}} + \frac{1}{1-S^2}[(\pi_u \bar{\pi}_u \mid \bar{\pi}_g \pi_g) + (\pi_u \pi_g \mid \bar{\pi}_g \bar{\pi}_u)] = \tag{15}$$
$$= \frac{1}{1-S^2}\{(x_A x_A \mid x_A x_A) - (x_A x_B \mid x_A x_B) + (x_A y_A \mid x_A y_A) - (x_A y_B \mid x_A y_B)\},$$
$$^3\Sigma_u^+ : J_{u\bar{g}} - K_{u\bar{g}} + \frac{1}{1-S^2}[(\pi_u \bar{\pi}_u \mid \bar{\pi}_g \pi_g) - (\pi_u \pi_g \mid \bar{\pi}_g \bar{\pi}_u)] =$$
$$= \frac{1}{1-S^2}\{(x_A x_A \mid x_B x_B) - (x_A x_B \mid x_A x_B) + (x_A y_A \mid x_B y_B) - (x_A y_B \mid x_B y_A)\},$$
$$^1\Sigma_u^- : J_{u\bar{g}} + K_{u\bar{g}} - \frac{1}{1-S^2}[(\pi_u \bar{\pi}_u \mid \bar{\pi}_g \pi_g) + (\pi_u \pi_g \mid \bar{\pi}_g \bar{\pi}_u)] =$$
$$= \frac{1}{1-S^2}\{(x_A x_A \mid y_B y_B) - (x_A x_B \mid y_A y_B) - (x_A y_A \mid x_B y_B) + (x_A y_B \mid x_A y_B)\},$$
$$^3\Sigma_u^- : J_{u\bar{g}} - K_{u\bar{g}} - \frac{1}{1-S^2}[(\pi_u \bar{\pi}_u \mid \bar{\pi}_g \pi_g) - (\pi_u \pi_g \mid \bar{\pi}_g \bar{\pi}_u)] =$$
$$= \frac{1}{1-S^2}\{(x_A x_A \mid y_A y_A) - (x_A x_B \mid y_A y_B) - (x_A y_A \mid x_A y_A) + (x_A y_B \mid x_B y_A)\}.$$

In Eq. (15), the "chemists' notation"[8] for four-center integrals is employed,

$$\iint a^*(1) b^*(2) \frac{1}{r_{12}} c(1) d(2) d\tau_1 d\tau_2 \equiv (a\, c \mid b\, d), \tag{16}$$

the Coulomb and exchange integrals are introduced

$$J_{ug} \equiv (u\,u \mid g\,g), \quad K_{ug} \equiv (u\,g \mid g\,u), \quad J_{u\bar{g}} \equiv (u\,u \mid \bar{g}\,\bar{g}), \quad K_{u\bar{g}} \equiv (u\,\bar{g} \mid \bar{g}\,u) \tag{17}$$

(where u denotes π_u and g π_g), and the matrix elements expressed also in terms of the atomic basis functions.

The values for the four-center integrals can be estimated by means of the Mulliken formula[9]:

$$(a\,b\,|\,c\,d) \approx \frac{1}{4} S_{ab} S_{cd} \left[(a\,a\,|\,c\,c) + (b\,b\,|\,c\,c) + (a\,a\,|\,d\,d) + (b\,b\,|\,d\,d)\right], \tag{18}$$

where S_{ab} and S_{cd} are overlap integrals for the orbitals a, b, and c, d, respectively. An analysis of the expressions (15) leads to the following ordering of the acetylene excited electronic states in order of increasing energy:

$$^3\Sigma_u^+,\ ^3\Delta_u,\ ^3\Sigma_u^-,\ ^1\Sigma_u^-,\ ^1\Delta_u,\ ^1\Sigma_u^+. \tag{19}$$

All these states except for $^1\Sigma_u^+$ (lying at very high energy) represent the lowest-lying excited species of the acetylene molecule.

The excited electronic states corresponding to the $\pi_u^3\,\pi_g$ electronic configurations are followed by a series of Rydberg-type states arising by excitations out of the π_u orbital into the orbitals involving the Rydberg AOs. The energy positions of these species generally match very reasonably the formula

$$T_R = IP - R/(n-\delta)^2 \tag{20}$$

where T_R is the term value of the state in question, IP the ionization potential of the molecule (11.4 eV), R the Rydberg constant, n the principal quantum number of the Rydberg state, and δ the quantum defect (usually assumed to be $\delta = 1.0$ for s series, $\delta = 0.4/0.5$ for p, and $\delta = 0.0/0.1$ for d states). The only exception represent the lowest-lying states of both singlet and triplet multiplicity (corresponding to the $1\pi_u \rightarrow 3s_R$ electron excitation) the vertical energies of which differ significantly from those obtained by means of formula 20, indicating that these species are of mixed Rydberg-valence character. The Rydberg states of acetylene converge towards the ground state, X $^2\Pi_u$, of the $C_2H_2^+$ ion.

TRANS-BENDING POTENTIAL CURVES

At *trans*-bent nuclear arrangements (point group C_{2h}), the π_u and π_g orbitals split into $3b_u + 1a_u$ and $4a_g + 1b_g$, respectively. One-electron excitations out of $3b_u$ ($\equiv b_u$) or $1a_u$ ($\equiv a_u$) into $4a_g$ ($\equiv a_g$) or $1b_g$ ($\equiv b_g$) lead to the electronic species represented by the following sixteen Slater determinants

$$\begin{aligned}
&D_1^T = |a_u\alpha, a_g\alpha|, D_2^T = |a_u\alpha, a_g\beta|, D_3^T = |a_u\alpha, b_g\alpha|, D_4^T = |a_u\alpha, b_g\beta|,\\
&D_5^T = |a_u\beta, a_g\alpha|, D_6^T = |a_u\beta, a_g\beta|, D_7^T = |a_u\beta, b_g\alpha|, D_8^T = |a_u\beta, b_g\beta|,\\
&D_9^T = |b_u\alpha, a_g\alpha|, D_{10}^T = |b_u\alpha, a_g\beta|, D_{11}^T = |b_u\alpha, b_g\alpha|, D_{12}^T = |b_u\alpha, b_g\beta|,\\
&D_{13}^T = |b_u\beta, a_g\alpha|, D_{14}^T = |b_u\beta, a_g\beta|, D_{15}^T = |b_u\beta, b_g\alpha|, D_{16}^T = |b_u\beta, b_g\beta|.
\end{aligned} \tag{21}$$

These Slater determinants are combined into "spectroscopically correct" electronic states, *i.e.*, species being eigenfunctions of the spin operators S^2 and S_z and belonging to a particular irrep of the C_{2h} point group as

$$
\begin{aligned}
1\ {}^1\mathrm{A_u} &= \frac{1}{\sqrt{2}}\,(D_2{}^{\mathrm{T}} - D_5{}^{\mathrm{T}}) = \frac{1}{\sqrt{2}}\,(\mathrm{a_u a_g} + \mathrm{a_g a_u})\,\Theta^1,\\
2\ {}^1\mathrm{A_u} &= \frac{1}{\sqrt{2}}\,(D_{12}{}^{\mathrm{T}} - D_{15}{}^{\mathrm{T}}) = \frac{1}{\sqrt{2}}\,(\mathrm{b_u b_g} + \mathrm{b_g b_u})\,\Theta^1;\\
1\ {}^3\mathrm{A_u}\,(M_s = 1) &= D_1{}^{\mathrm{T}} = \frac{1}{\sqrt{2}}\,(\mathrm{a_u a_g} - \mathrm{a_g a_u})\,\Theta_1{}^3,\\
1\ {}^3\mathrm{A_u}\,(M_s = 0) &= \frac{1}{\sqrt{2}}\,(D_2{}^{\mathrm{T}} + D_5{}^{\mathrm{T}}) = \frac{1}{\sqrt{2}}\,(\mathrm{a_u a_g} - \mathrm{a_g a_u})\,\Theta_0{}^3,\\
1\ {}^3\mathrm{A_u}\,(M_s = -1) &= D_6{}^{\mathrm{T}} = \frac{1}{\sqrt{2}}\,(\mathrm{a_u a_g} - \mathrm{a_g a_u})\,\Theta_{-1}{}^3;\\
2\ {}^3\mathrm{A_u}\,(M_s = 1) &= D_{11}{}^{\mathrm{T}} = \frac{1}{\sqrt{2}}\,(\mathrm{b_u b_g} - \mathrm{b_g b_u})\,\Theta_1{}^3,\\
2\ {}^3\mathrm{A_u}\,(M_s = 0) &= \frac{1}{\sqrt{2}}\,(D_{12}{}^{\mathrm{T}} + D_{15}{}^{\mathrm{T}}) = \frac{1}{\sqrt{2}}\,(\mathrm{b_u b_g} - \mathrm{b_g b_u})\,\Theta_0{}^3,\\
2\ {}^3\mathrm{A_u}\,(M_s = -1) &= D_{16}{}^{\mathrm{T}} = \frac{1}{\sqrt{2}}\,(\mathrm{b_u b_g} - \mathrm{b_g b_u})\,\Theta_{-1}{}^3,\\
1\ {}^1\mathrm{B_u} &= \frac{1}{\sqrt{2}}\,(D_4{}^{\mathrm{T}} - D_7{}^{\mathrm{T}}) = \frac{1}{\sqrt{2}}\,(\mathrm{a_u b_g} + \mathrm{b_g a_u})\,\Theta^1,\\
2\ {}^1\mathrm{B_u} &= \frac{1}{\sqrt{2}}\,(D_{10}{}^{\mathrm{T}} - D_{13}{}^{\mathrm{T}}) = \frac{1}{\sqrt{2}}\,(\mathrm{b_u a_g} + \mathrm{a_g b_u})\,\Theta^1,\\
1\ {}^3\mathrm{B_u}\,(M_s = 1) &= D_3{}^{\mathrm{T}} = \frac{1}{\sqrt{2}}\,(\mathrm{a_u b_g} - \mathrm{b_g a_u})\,\Theta_1{}^3,\\
1\ {}^3\mathrm{B_u}\,(M_s = 0) &= \frac{1}{\sqrt{2}}\,(D_4{}^{\mathrm{T}} + D_7{}^{\mathrm{T}}) = \frac{1}{\sqrt{2}}\,(\mathrm{a_u b_g} - \mathrm{b_g a_u})\,\Theta_0{}^3;\\
1\ {}^3\mathrm{B_u}\,(M_s = -1) &= D_8{}^{\mathrm{T}} = (\mathrm{a_u b_g} - \mathrm{b_g a_u})\,\Theta_{-1}{}^3,\\
2\ {}^3\mathrm{B_u}\,(M_s = 1) &= D_9{}^{\mathrm{T}} = \frac{1}{\sqrt{2}}(\mathrm{b_u a_g} - \mathrm{a_g b_u})\,\Theta_1{}^3,\\
2\ {}^3\mathrm{B_u}\,(M_s = 0) &= \frac{1}{\sqrt{2}}\,(D_{10}{}^{\mathrm{T}} + D_{13}{}^{\mathrm{T}}) = \frac{1}{\sqrt{2}}\,(\mathrm{b_u a_g} - \mathrm{a_g b_u})\,\Theta_0{}^3,\\
2\ {}^3\mathrm{B_u}\,(M_s = -1) &= D_{14}{}^{\mathrm{T}} = \frac{1}{\sqrt{2}}(\mathrm{b_u a_g} - \mathrm{a_g b_u})\,\Theta_{-1}{}^3.
\end{aligned}
\tag{22}
$$

The MOs in the $D_{\infty,\mathrm{h}}$ point group are connected with their $C_{2\mathrm{h}}$ counterparts by the relations

$$
\begin{aligned}
\pi_{\mathrm{u}} &= \frac{1}{\sqrt{2}}\,(\mathrm{b_u} + \mathrm{i}\ \mathrm{a_u}), \quad \bar{\pi}_{\mathrm{u}} = \frac{1}{\sqrt{2}}\,(\mathrm{b_u} - \mathrm{i}\ \mathrm{a_u}),\\
\pi_{\mathrm{u}} &= \frac{1}{\sqrt{2}}\,(\mathrm{a_g} + \mathrm{i}\ \mathrm{b_g}), \quad \bar{\pi}_{\mathrm{u}} = \frac{1}{\sqrt{2}}\,(\mathrm{a_g} - \mathrm{i}\ \mathrm{b_g}).
\end{aligned}
\tag{23}
$$

By using (23), the correlation between the electronic states of the two point groups considered can be derived. It reads

$$\begin{aligned}
\frac{1}{\sqrt{2}}\,({}^1\Delta_u + {}^1\overline{\Delta}_u) &\rightarrow \frac{1}{\sqrt{2}}(2^1B_u - 1^1B_u),\\
\frac{1}{\sqrt{2}}\,({}^1\Delta_u - {}^1\overline{\Delta}_u) &\rightarrow \frac{i}{\sqrt{2}}(2^1A_u - 1^1A_u),\\
\frac{1}{\sqrt{2}}\,({}^3\Delta_u + {}^3\overline{\Delta}_u) &\rightarrow \frac{1}{\sqrt{2}}(1^3B_u - 2^3B_u),\\
\frac{1}{\sqrt{2}}\,({}^3\Delta_u - {}^3\overline{\Delta}_u) &\rightarrow \frac{i}{\sqrt{2}}(2^3A_u + 1^3A_u),\\
{}^1\Sigma_u^+ &\rightarrow \frac{1}{\sqrt{2}}\,(2^1B_u + 1^1B_u),\\
{}^1\Sigma_u^- &\rightarrow \frac{i}{\sqrt{2}}\,(1^1A_u - 2^1A_u),\\
{}^3\Sigma_u^+ &\rightarrow \frac{1}{\sqrt{2}}\,(1^3B_u - 2^3B_u),\\
{}^3\Sigma_u^- &\rightarrow \frac{i}{\sqrt{2}}\,(1^3A_u - 2^3A_u).
\end{aligned} \tag{24}$$

The geometry of the electronic states of acetylene in terms of the energy change of the MOs involved in the corresponding wave functions upon *trans*-bending are now discussed. Only the singlet electronic states will be considered – the analysis of triplet species can be carried out in a completely analogous way. At the linear nuclear arrangement, the electronic configuration of the ground electronic state of acetylene, $X^1\Sigma_g^+$ is ... π_u^4. At *trans*-bent geometries it becomes ... $3b_u^2 1a_u^2$. The effect of decreasing the energy of the $3b_u^2$ orbital upon bending is outweighed by the strong energy increase of the $3a_g$ MO (also doubly occupied), resulting in a linear equilibrium geometry of the $X^1\Sigma_g^+$ state. The correlation scheme given by Eqs. (24) shows that the first excited singlet state, ${}^1\Sigma_u^-$, correlates with the antisymmetric linear combination of the 1^1A_u and 2^1A_u species of the C_{2h} point group, with coefficients of exactly equal magnitude ($1/\sqrt{2}$). However, already at small distortions from linearity, the 1^1A_u component becomes dominant. The ${}^1\Delta_u$ electronic state of the linear molecule splits upon bending into a B_u and a A_u component (the Renner-Teller effect[10]). The B_u component retains also at *trans*-bent geometries the composition given by the first of Eqs. (24), on the other hand the 2^1A_u species become dominant in the A_u component of the $1\Delta_u$ state. The composition of the two lowest-lying singlet electronic states of A_u symmetry can be interpreted as mixing of the ${}^1\Sigma_u^-$ and ${}^1\Delta_u$ states at *trans*-bent geometries. The mixing between the B_u component of the ${}^1\Delta_u$ state and the species of the same symmetry (B_u) correlating with the ${}^1\Sigma_u^+$ state of the linear molecule is not significant (at least at small distortions from linearity), because of a relatively large energy difference between the ${}^1\Sigma_u^+$ and ${}^1\Delta_u$ states.

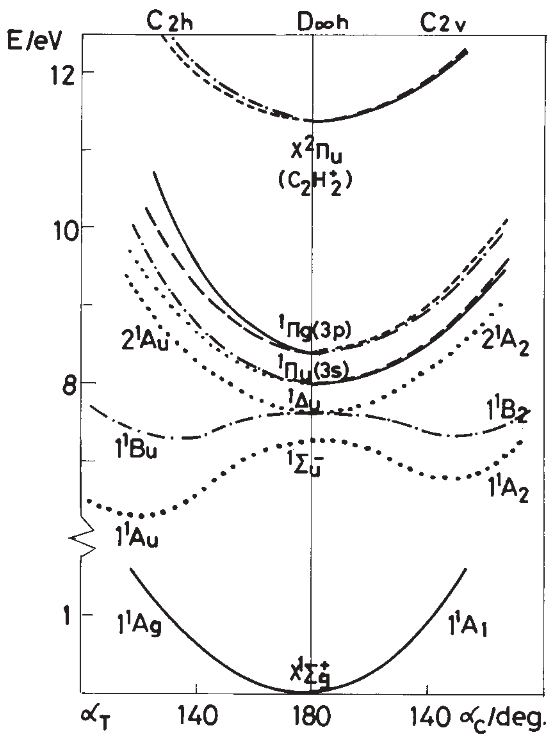

Fig. 2. *Trans* (left-hand side) and *cis*- (right-hand side) bending potential curves for singlet electronic states of acetylene. Solid lines: states A_g (C_{2h} point group) and A_1 (C_{2v} group) symmetry; dotted lines A_u and A_2 states; dashed lines B_g and B_1; dash-dotted lines: B_u and B_2 species.

The fact that the state correlating with $^1\Sigma_u^-$ (see Eqs. (22)) corresponds to the excitation from the $1a_u$ orbital, the energy of which does not change significantly upon bending, into $4a_g$, being stabilized at bent geometries (see Fig. 1a), has as a consequence the geometry of this electronic state being bent at equilibrium. On the other hand, the A_u component of the $^1\Delta_u$ state corresponds to the excitation from the $3b_u$ orbital, the energy of which decreases upon bending, into $1b_g$, with an energy practically independent of variation in the geometry; this leads to a continuous increase of the energy for the electronic state in question with increasing distortion from linearity. The other component of the $^1\Delta_u$ state (of B_u symmetry) is described by two leading configurations corresponding to $3b_u \rightarrow 4a_g$, $1a_u \rightarrow 1b_g$ excitations with respect to the ground state. Inspection of Fig. 1a shows that it is difficult to predict precisely whether linear or bent geometry will be preferred by an electronic state of such a composition; the results of explicit *ab initio* computations (Fig. 2, Refs. 11–13) show that it is non-linear, but with a very flat potential curve.

Rydberg electronic states arise by excitations out of the orbitals $1a_u$ and $3b_u$, correlating with π_u, into the MOs involving Rydberg-type AOs. Since the latter show negligible dependence on the molecular geometry, all Rydberg states possess linear equilibrium geometry. The states arising by excitations out of the $1a_u$ MO lie below those corresponding to excitations from its lower-energy counterpart $3b_u$, as, for example, the A_u component of the first singlet Rydberg state, $1^1\Pi_u$ [$1a_u \rightarrow 3s_R(a_g)$ excitation] with respect to the B_u component [$3b_u \rightarrow 3s_R(a_g)$ excitation] of the same state (see Fig. 2).

CIS-BENDING POTENTIAL CURVES

At *cis*-bent molecular geometries (point group $C_{2\upsilon}$), the π_u and π_g orbitals split into $1b_1$+$4a_1$ and $3b_2$+$1a_2$, respectively. One-electron excitations out of $1b_1$ ($\equiv b_1$) or $4a_1$($\equiv a_1$) into $3b_2$ ($\equiv b_2$) or $1a_2$ ($\equiv a_2$) lead to the electronic species represented by the following sixteen Slater determinants

$$\begin{aligned}
&D_1{}^C = |a_1\,\alpha, b_2\,\alpha|, D_2{}^C = |a_1\,\alpha, b_2\,\beta|, D_3{}^C = |a_1\,\alpha, a_2\,\alpha|, D_4{}^C = |a_1\,\alpha, a_2\,\beta|,\\
&D_5{}^C = |a_1\,\beta, b_2\,\alpha|, D_6{}^C = |a_1\,\beta, b_2\,\beta|, D_7{}^C = |a_1\,\beta, a_2\,\alpha|, D_8{}^C = |a_1\,\beta, a_2\,\beta|,\\
&D_9{}^C = |b_1\,\alpha, b_2\,\alpha|, D_{10}{}^C = |b_1\,\alpha, b_2\,\beta|, D_{11}{}^C = |b_1\,\alpha, a_2\,\alpha|, D_{12}{}^C = |b_1\,\alpha, a_2\,\beta|,\\
&D_{13}{}^C = |b_1\,\beta, b_2\,\alpha|, D_{14}{}^C = |b_1\,\beta, b_2\,\beta|, D_{15}{}^C = |b_1\,\beta, a_2\,\alpha|, D_{16}{}^C = |b_1\,\beta, a_2\,\beta|.
\end{aligned} \tag{25}$$

The spectroscopic states built by linear combinations of the determinants (25) are

$$\begin{aligned}
1\,{}^1A_2 &= \frac{1}{\sqrt{2}}(D_4{}^C - D_7{}^C) = \frac{1}{\sqrt{2}}(a_1a_2 + a_2a_1)\,\Theta^1,\\
2\,{}^1A_2 &= \frac{1}{\sqrt{2}}(D_{10}{}^C - D_{13}{}^C) = \frac{1}{\sqrt{2}}(b_1b_2 + b_2b_1)\,\Theta^1;\\
1\,{}^3A_2\,(M_s = 1) &= D_3{}^C = \frac{1}{\sqrt{2}}(a_1a_2 - a_2a_1)\,\Theta_1{}^3,\\
1\,{}^3A_2\,(M_s = 0) &= \frac{1}{\sqrt{2}}(D_4{}^C - D_7{}^C) = \frac{1}{\sqrt{2}}(a_1a_2 - a_2a_1)\,\Theta_0{}^3,\\
1\,{}^3A_2\,(M_s = -1) &= D_8{}^C = \frac{1}{\sqrt{2}}(a_1a_2 - a_2a_1)\,\Theta_{-1}{}^3;\\
2\,{}^3A_2\,(M_s = 1) &= D_9{}^C = \frac{1}{\sqrt{2}}(b_1b_2 - b_2b_1)\,\Theta_1{}^3,\\
2\,{}^3A_2\,(M_s = 0) &= \frac{1}{\sqrt{2}}(D_{10}{}^C + D_{13}{}^C) = \frac{1}{\sqrt{2}}(b_1b_2 - b_2b_1)\,\Theta_0{}^3,\\
2\,{}^3A_2\,(M_s = -1) &= D_{14}{}^C = \frac{1}{\sqrt{2}}(b_1b_2 - b_2b_1)\,\Theta_{-1}{}^3,\\
1\,{}^1B_2 &= \frac{1}{\sqrt{2}}(D_2{}^C - D_5{}^C) = \frac{1}{\sqrt{2}}(a_1b_2 + b_2a_1)\,\Theta^1,\\
2\,{}^1B_2 &= \frac{1}{\sqrt{2}}(D_{12}{}^C - D_{15}{}^C) = \frac{1}{\sqrt{2}}(b_1a_2 + a_2b_1)\,\Theta^1,\\
1\,{}^3B_2\,(M_s = 1) &= D_1{}^C = \frac{1}{\sqrt{2}}(a_1b_2 - b_2a_1)\,\Theta_1{}^3;\\
1\,{}^3B_2\,(M_s = 0) &= \frac{1}{\sqrt{2}}(D_2{}^C + D_5{}^C) = \frac{1}{\sqrt{2}}(a_1b_2 - b_2a_1)\,\Theta_0{}^3;\\
1\,{}^3B_2\,(M_s = -1) &= D_6{}^C = (a_1b_2 - b_2a_1)\,\Theta_{-1}{}^3;\\
2\,{}^3B_2\,(M_s = 1) &= D_{11}{}^C = \frac{1}{\sqrt{2}}(b_1a_2 - a_2b_1)\,\Theta_1{}^3;\\
2\,{}^3B_2\,(M_s = 0) &= \frac{1}{\sqrt{2}}(D_{12}{}^C + D_{15}{}^C) = \frac{1}{\sqrt{2}}(b_1a_2 - a_2b_1)\,\Theta_0{}^3;\\
2\,{}^3B_2\,(M_s = -1) &= D_{16}{}^C = \frac{1}{\sqrt{2}}(b_1a_2 - a_2b_1)\,\Theta_{-1}{}^3.
\end{aligned} \tag{26}$$

The MOs in the $D_{\infty h}$ point group are connected with those of the C_{2h} by the relations

$$\begin{aligned}\pi_u &= \frac{1}{\sqrt{2}}(a_1 + i\,b_1), \quad \bar{\pi}_u = \frac{1}{\sqrt{2}}(a_1 - i\,b_1)\\ \pi_g &= \frac{1}{\sqrt{2}}(b_2 + i\,a_2), \quad \bar{\pi}_g = \frac{1}{\sqrt{2}}(b_2 - i\,a_2).\end{aligned} \tag{27}$$

The states of the $D_{\infty h}$ and $C_{2\upsilon}$ point groups correlate with one another in the following way:

$$\begin{aligned}\frac{1}{\sqrt{2}}({}^1\Delta_u + {}^1\bar{\Delta}_u) &\to \frac{1}{\sqrt{2}}(1^1B_2 - 2^1B_2),\\ \frac{1}{\sqrt{2}}({}^1\Delta_u - {}^1\bar{\Delta}_u) &\to \frac{i}{\sqrt{2}}(2^1A_2 + 1^1A_2),\\ \frac{1}{\sqrt{2}}({}^3\Delta_u + {}^3\bar{\Delta}_u) &\to \frac{1}{\sqrt{2}}(1^3B_2 - 2^3B_2),\\ \frac{1}{\sqrt{2}}({}^3\Delta_u - {}^3\bar{\Delta}_u) &\to \frac{i}{\sqrt{2}}(2^3A_2 + 1^3A_2),\\ {}^1\Sigma_u^+ &\to \frac{1}{\sqrt{2}}(2^1B_2 + 1^1B_2),\\ {}^1\Sigma_u^- &\to \frac{i}{\sqrt{2}}(1^1A_2 - 2^1A_2),\\ {}^3\Sigma_u^+ &\to \frac{1}{\sqrt{2}}(1^3B_2 + 2^3B_2),\\ {}^3\Sigma_u^- &\to \frac{i}{\sqrt{2}}(1^3A_2 - 2^3A_2).\end{aligned} \tag{28}$$

Again only singlet electronic states will be discussed. The energy of the state correlating with the X ${}^1\Sigma_g^+$ linear species, ... $1b_1^2 4a_2^2$, increases upon *cis*-bending. In analogy with the situation at *trans*-bending, the first excited singlet state (${}^1\Sigma_u^-$ at linear geometry) is at *cis*-bent geometries predominantly described by the single 1^1A_2 wave function ($1b_1 \rightarrow 3b_2$ excitation with respect to the ground state), and the component of the ${}^1\Delta_u$ state of the same symmetry by 2^1A_2 ($4b_1 \rightarrow 1a_2$ excitation). The other ${}^1\Delta_u$ component (of B_2 symmetry) retains the composition it has at linear geometry ($4a_1 \rightarrow 3b_2$, $1b_1 \rightarrow 1a_2$). Reasoning analogous to that carried out for *trans*-bending leads to the conclusion that the first singlet state of A_2 symmetry (correlating with ${}^1\Sigma_u^-$) has bent equilibrium geometry, while the second A_2 species (which correlates with ${}^1\Delta_u$) prefers linear geometry. The lowest-lying B_1 state (the other ${}^1\Delta_u$ component) is slightly non-linear, like its B_u *trans*-planar counterpart. All Rydberg-type species are predicted to be more stable at linear geometry than at *cis*-planar nuclear arrangements.

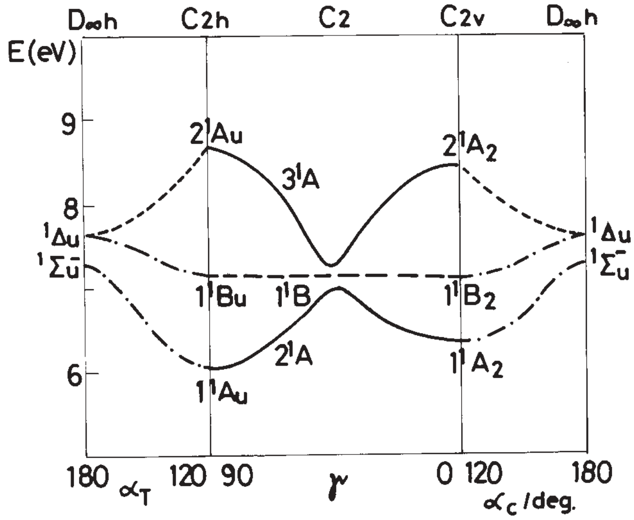

Fig. 3. Torsional potential curves for low-lying excited singlet states of acetylene corresponding to a H–C–C bond angle of 120º (central part of the figure). On the left-hand side of the figure the *trans*-bending curves for the interval of ∠ H–C–C values between 180º (linear geometry) and 120º is reproduced. Right-hand side: *cis*-bending curves.

TORSIONAL POTENTIAL CURVES

The dependence of the energy of the MOs on the torsional angle, presented in Fig. 1b, is directly reflected in the form of the potential curves for torsional motion. The lowest-energy potential curve corresponds to the electronic configuration ... $3b^2\ 4a^2$, 1^1A. This state corresponds at *trans*-planar geometry to 1^1A_g and at *cis*-planar nuclear arrangement to 1^1A_1, both of these species correlating with the $X^1\Sigma_g^+$ state of the linear molecule. A consequence of the very weak torsional dependence of all the MOs involved in the wave function of the 1^1A state is that the corresponding potential curve has the form of a nearly straight line. On the other hand, the composition and energy of the next two ^1A electronic states in order of increasing energy show dramatic changes upon torsion. The lower-energy one of them correlates at *trans*-planar geometry with the ... $3b_u^2\ 1a_u\ 4a_g$, 1^1A_u species and at *cis*-planar geometry with ... $1b_1\ 4a_1^2\ 3b_2$, 1^1A_2. This means that at large values of the torsional angle γ (*i.e.*, at relatively small torsional distortions with respect to the *trans*-planar geometry) the electronic configuration for the 2^1A electronic state is ... $3b^2$ 4a 5a (4a→5a electronic excitation with respect to the 1^1A state), and at small γ values (nearly *cis*-planar geometry) it is ... 3b $4a^2$ 4b (3b→4b electronic excitation with respect to the 1^1A state). This change in the composition of the wave functions for the 2^1A adiabatic state is easily understandable in terms of the MO diagram presented in Fig. 1b: At large γ values, the 4a→5a excitation is energetically more favorable than 3b→4b, while the situation is opposite for small values of γ. The behavior of the 3^1A state is complemental to that of its 2^1A counterpart. This leads to an "avoided crossing" of the 2^1A and 3^1A adiabatic potential curves and consequently to a potential barrier for the 2^1A state at $\gamma \approx \pi/4$. On the other hand, the torsional potential curve for the 1^1B state, connecting with each other the 1^1B_u (C_{2h} geometry) and 1^1B_2 ($C_{2\upsilon}$) states, has a relatively monotonous form. This concerns also all the Rydberg-type electronic states. In Fig. 3 are displayed the *ab initio* computed torsional curves for the 2^1A, 3^1A and 1^1B electronic states.[12] They confirm the above analysis. It should be noted, however, that *ab initio* calculations showed that the electronic states in question are at non-planar geometries appreciably admixed by Rydberg-type MOs.

ELECTRONIC SPECTRA OF ACETYLENE

At linear nuclear arrangement, representing the equilibrium geometry of the ground state $X^1\Sigma_g^+$ of acetylene, electronic transitions to all low-lying valence-type excited states $^3\Sigma_u^+$, $^3\Delta_u$, $^3\Sigma_u^-$, $^1\Sigma_u^-$ and $^1\Delta_u$ are forbidden. The lowest-energy dipole allowed transition in absorption involves the first member of the singlet Rydberg series, $^1\Pi_u(3s_R)$. For this reason the majority of the experimental studies have been devoted to the investigation of the Rydberg spectrum of acetylene (for a historical overview see Ref. 13). However, when the linear molecular geometry is distorted, many of the "vertically forbidden" transitions become allowed. The first excited singlet state ($^1\Sigma_u^-$ at linear geometry) correlates with the 1^1A_u species at C_{2h} geometry and with 1^1A_2 at $C_{2\upsilon}$. While the electronic transition from the ground state (1^1A_g at C_{2h}, 1^1A_1 at $C_{2\upsilon}$) to the latter species remains forbidden, the $1^1A_g \rightarrow 1^1A_u$ transition at *trans*-planar geometry is allowed. However, such a "non-vertical" transition is of low intensity.[14–16] The spectrum arising from a transition into the 1^1B_u state, correlating at the linear geometry with $^1\Delta_u$ has also been observed.[17–19] It is possible that some of the features ascribed to this spectrum originate from the transition into the B_2 component of the $^1\Delta_u$ state (see, *e.g.*, Ref. 12). On the other hand, the transition from the ground state into the A_2 component of $^1\Delta_u$ is forbidden, and the spectrum involving the A_u component of $^1\Delta_u$, preferring linear geometry, should be extremely weak.

CONCLUSION

In the present study it has been shown that all the global features of the electronic spectra of acetylene can be reproduced by means of the group theory, combined with elementary quantum chemical considerations, based ultimately on an inspection of the composition of a set of low-energy molecular orbitals. The reliability of this analysis is confirmed by comparison with the results of explicit *ab initio* calculations on the same system,[11,12] as well as with the available experimental findings. Moreover, with minor modifications, this approach can be used to predict the structure of spectra for a number of related species, for example $C_2H_2^+$, B_2H_2, $B_2H_2^+$, as documented in Ref. 13.

Acknowledgements: We thank the Ministry of Science, Technology and Development of the Republic of Serbia for financial support.

ИЗВОД

КОРИШЋЕЊЕ ТЕОРИЈЕ ГРУПА ЗА КЛАСИФИКАЦИЈУ ЕЛЕКТРОНСКИХ СТАЊА АЦЕТИЛЕНА

СТАНКА ЈЕРОСИМИЋ и МИЉЕНКО ПЕРИЋ

Факултет за физичку хемију, Универзитет у Београду, Студентски трг 16, 11000 Београд

Електронска стања молекула ацетилена класификована су коришћењем теорије група у комбинацији са Волшовим дијаграмима и неким елементарним квантнохемијским разматрањима. Показано је да се глобална структура електронског спектра може репродуковати/предвидети и без детаљних квантнохемијских рачуна.

(Примљено 15. јула 2002)

REFERENCES

1. F. A. Cotton, *Chemical Applications of Group Theory*, Wiley-Interscience, New York (1971)
2. P. R. Bunker, *Molecular Symmetry and Spectroscopy*, Academic Press, New York, San Francisco, London (1979)
3. R. S. Mulliken, *Rev. Mod. Phys.* **14** (1942) 204; *Can. J. Chem.* **36** (1958) 10
4. A. D. Walsh, *J. Chem. Soc.* (1953), 2260, 2266, 2288, 2296, 2301, 2306
5. R. J. Buenker, S. D. Peyerimhoff, *Chem. Rev.* **74** (1974) 127
6. W. Kutzelnigg, *Einführung in die theoretische Chemie*, Verlag Chemie, Weinheim - New York (1978)
7. M. Perić, B. Ostojić, *J. Serb. Chem. Soc.* **62** (1997) 817
8. A. Szabo, N. S. Ostlund, *Modern Quantum Chemistry*, Dover Publications, Mineola, New York (1989)
9. R. S. Mulliken, *J. Chim. Phys.* **46** (1949) 497
10. R. Renner, *Z. Phys.* **92** (1934) 172
11. M. Perić, R. J. Buenker, S. D. Peyerimhoff, *Mol. Phys.* **53** (1984) 1177
12. M. Perić, S. D. Peyerimhoff, R. J. Buenker, *Mol. Phys.* **62** (1987) 1339
13. M. Perić, S. D. Peyerimhoff, *The Role of Rydberg States in Spectroscopy and Photochemistry*, C. Sandorfy, Ed., Kluwer Academic Publishers, Dordrecht, Boston, London (1999), p. 137
14. C. K. Ingold, G. W. King, *Nature, London* **169** (1952) 1101
15. C. K. Ingold, G. W. King, *J. Chem. Soc.* (1953) 2702
16. K. K. Innes, *J. Chem. Phys.* **22** (1954) 863
17. G. Herzberg, *Discuss. Faraday Soc.* **35** (1963) 7
18. P. G. Wilkinson, *J. Mol. Spectrosc.* **2** (1958) 387
19. P. D. Foo, K. K. Innes, *Chem. Phys. Lett.* **22** (1973) 439.